

Study of local properties of fibre Bragg gratings by the method of optical space-domain reflectometry

I.G. Korolev, S.A. Vasil'ev, O.I. Medvedkov, E.M. Dianov

Abstract. The method of optical space-domain reflectometry for measuring local spatial characteristics of fibre Bragg gratings (FBGs) is described in detail. It is demonstrated experimentally that, by using IR and UV radiation sources, this method provides good sensitivity ($\sim 10^{-4}$) of measuring the modulation amplitude of the induced refractive index in the core of an optical fibre and a high spatial resolution ($\sim 100 \mu\text{m}$ and better). The factors affecting the accuracy of measurements as well as technical and methodological limitations of the method are considered. A comparative analysis of modern methods for studying the spatial properties of FBGs is performed and applications of these methods are considered.

Keywords: optical fibre, fibre Bragg grating, space-domain reflectometry, methods for studying fibre gratings.

1. Introduction

Fibre Bragg gratings (FBGs) are widely used in fibre lasers and amplifiers, in fibre systems for measuring physical quantities, optical communication lines, etc. Numerous applications of fibre gratings are considered, for example, in reviews [1, 2].

A fibre grating represents a longitudinal, periodic variation in the refractive index in the core of an optical fibre. The main parameters of the grating are the distributions of the amplitude and period of the refractive index modulation, as well of the average value of the induced refractive index along the fibre axis. These parameters specify the spectral and dispersion properties of gratings and, thus, determine their use in different applications of the fibre optics.

Because the typical period of a FBG is $\sim 0.5 \mu\text{m}$, gratings are produced, as a rule, using the interferometric methods by illuminating a fibre through its side surface. Usually FBGs are produced by exposing an optical fibre to UV radiation (from excimer lasers, the second harmonic of an argon laser, etc.) at the wavelengths where a linear absorption of a doped glass of the fibre core is sufficiently

high ($\sim 10 - 100 \text{ dB cm}^{-1}$). Germanosilica fibres, which have the absorption bands of germanium oxygen-deficient centres, are commonly used for this purpose [3]. Along with germanosilica fibres, other photosensitive glasses are also available (see references in paper [4]). In addition, the UV sensitivity of glasses can be enhanced using special procedures, of which the most popular is the loading of the glass network with hydrogen [5].

A diversity of the types of gratings developed at present is explained by their numerous applications. For example, in the case of Raman converters, gratings with the high ($R > 99.9\%$) and low ($R \sim 5\% - 10\%$) reflection coefficients are used [6, 7]. To compensate for the dispersion in optical fibres in communication lines [8], FBGs with a variable period are used, which have specified dispersion properties. To suppress the sidelobes in the transmission and reflection spectra of a grating, which is important in WDM communication systems, the amplitude of the refractive-index modulation is profiled in a special way (see Ch. 5 in Ref. [1]). When a FBG is used as a narrow-band transmission filter, the grating is fabricated with a certain phase shift [9]. All these and many other applications require the calculated parameters of gratings to be realised in practice with a high accuracy.

Therefore, the measurement of the characteristics (transmission and reflection spectra, dispersion, space-domain distribution of the induced refractive index) of gratings produced in an optical fibre is important for the choice and optimisation of FBG production methods, as well as for the analysis and correction of errors in written FBGs.

In this paper, we present a comparative review of the methods for studying parameters of FBGs. The theoretical and experimental aspects of one of the most universal methods, the method of optical space-domain reflectometry (OSDR), are discussed in detail. The advantages of this method are the high sensitivity and reproducibility of measurements, as well as a broad range of parameters being detected. The use of UV and IR radiations considerably simplifies the method and improves its characteristics.

2. Methods for studying the local properties of gratings

A FBG couples the counterpropagating modes of the core of a single-mode fibre. The efficient mode coupling is provided by the phase matching condition

$$2\beta = K, \quad (1)$$

I.G. Korolev, S.A. Vasil'ev, O.I. Medvedkov, E.M. Dianov Fiber Optics Research Center, A.M. Prokhorov General Physics Institute, Russian Academy of Sciences, ul. Vavilova 38, 119991 Moscow, Russia; fax: (095) 135-81-39

Received 11 April 2003

Kvantovaya Elektronika 33(8) 704–710 (2003)

Translated by M.N. Sapozhnikov

where $\beta = 2\pi n_{\text{eff}}/\lambda$ is the propagation constant of a mode; n_{eff} is the effective refractive index of a fibre mode; λ is the wavelength of light in vacuum; $K = 2\pi/\Lambda$ is the grating constant; and Λ is the grating period. In the general case of gratings with parameters variable over the grating length, condition (1) can be written in the form

$$\lambda_{\text{Br}}(z) = 2n_{\text{eff}}(z)\Lambda(z), \quad (2)$$

where λ_{Br} is the Bragg wavelength. The dependences n_{eff} and $\Lambda(z)$ mean that the corresponding quantities are averaged in the vicinity of the longitudinal coordinate z . Because absorption of UV radiation over the distance of the order of the fibre core diameter (5–10 μm) is, as a rule, weak, the induced refractive index is assumed constant along the core radius. Taking this into account, a change Δn_{ind} in the refractive index in the fibre core is related to a change Δn_{eff} in the effective refractive index of the fundamental mode by the expression

$$\Delta n_{\text{eff}} = \eta \Delta n_{\text{ind}}, \quad (3)$$

where

$$\eta = \int_0^a \int_0^{2\pi} EE^* r dr d\varphi \left(\int_0^\infty \int_0^{2\pi} EE^* r dr d\varphi \right)^{-1}$$

is the fraction of the power propagating in the fibre core of radius a and $E(r, \varphi)$ is the distribution of the electric field of the fundamental mode in cylindrical coordinates r and φ . For a step-indexed fibre, η is ~ 0.8 at the cut-off wavelength of the first higher mode.

A longitudinal periodic variation in the refractive index induced in the core of an optical fibre can be described as

$$\Delta n_{\text{ind}}(z) = \Delta n_{\text{avr}}(z) + \Delta n_{\text{mod}}(z) \frac{\exp[-i\theta(z)] + \text{c.c.}}{2}, \quad (4)$$

where $\Delta n_{\text{avr}}(z)$ and $\Delta n_{\text{mod}}(z)$ are the average value of the modulation of the induced refractive index and its amplitude, respectively. The phase in Eqn (4) is usually expressed in terms of the averaged period of the grating A_0 : $\theta(z) = 2\pi z/A_0 + \varphi(z)$, where $\varphi(z)$ are relatively small, compared to the first term, variations in the phase. It is convenient to choose the period A_0 that corresponds to the central wavelength λ_0 in the reflection spectrum of the grating. In this case, $\lambda_0 = 2\eta(n_0 + \bar{\Delta n})A_0$, where n_0 is the refractive index of the unperturbed core and $\bar{\Delta n}$ is the average induced refractive index. When the period of a grating depends on z , the phase in (4) is described by the expression $\theta(z) = 2\pi z/\Lambda(z)$.

The interaction of counterpropagating modes on the grating is described by the system of equations for coupled modes [10]

$$\frac{dA(z)}{dz} = -i\kappa(z)B(z), \quad (5)$$

$$\frac{dB(z)}{dz} = i\kappa^*(z)A(z),$$

where $A(z)$ and $B(z)$ are the wave amplitudes slowly varying at the wavelength scale for the waves propagating in the forward and backward directions, respectively; $\kappa(z) = |\kappa(z)| \exp[-i\phi_\kappa(z)]$ in the complex coupling coefficient of the grating.

The modulus $|\kappa(z)|$ of the coupling coefficient at the wavelength λ is proportional to the modulation amplitude of the induced refractive index:

$$|\kappa(z)| = \pi\eta\Delta n_{\text{mod}}(z)/\lambda. \quad (6)$$

The phase $\phi_\kappa(z)$ is determined by the integral of frequency detuning from phase matching (1)

$$\phi_\kappa(z) = \int_0^z [2\beta(z') - K(z')] dz'. \quad (7)$$

If $\Delta\lambda \ll \lambda_0$ and $\delta A \ll A_0$, then it follows from (7) that the derivative of the phase is related to the grating parameters by the expression

$$\frac{d\phi_\kappa(z)}{dz} \approx 2\pi \left[-\frac{\Delta\lambda}{A_0\lambda_0} + \frac{2\eta\delta n_{\text{ind}}(z)}{\lambda_0} + \frac{\delta A(z)}{A_0^2} \right], \quad (8)$$

where $\Delta\lambda = \lambda_{\text{meas}} - \lambda_0$ is the spectral detuning from the wavelength λ_{meas} at which the grating parameters are measured; and $\delta n_{\text{ind}}(z) = \Delta n_{\text{avr}}(z) - \bar{\Delta n}$ and $\delta A(z) = A(z) - A_0$ are the deviations of local values of the average induced refractive index and period, respectively.

In the general case the analysis of FBGs includes the solution of the direct and inverse problems. The solution of the direct problem consists in the determination of the spectral and dispersion characteristics of the grating from the known values of $\kappa(z)$. The inverse problem involves the determination of $\kappa(z)$ from the known spectral (and sometimes dispersion) parameters of the FBG.

The direct problem is widely used to simulate gratings numerically and to study the influence of various factors (phase shift, longitudinal refractive index profile, and grating period) on the FBG properties. When $\kappa(z)$ is known, the transmission and reflection spectra, as well as group delays of FBGs can be calculated by solving numerically the system of equations (5) even in the case of a complicated space-domain dependence of the coupling coefficient [10].

The solution of the inverse problem is also of great interest. However, it is much more complicated and time consuming. This is explained by the fact the transmission and reflection spectra are integrated characteristics of the grating, from which it is impossible to determine the space-domain distribution $\kappa(z)$ in the general case.

The methods of numerical solution of the inverse problem for FBGs were considered in papers [11–14]. These methods are separated into three main groups: the Fourier transform of a spectral response [14] and the solution of the backscattering problem with the help of integral (Gelfand–Levitan–Marchenko method [15]) and differential (layer-peeling algorithm [13]) equations. The layer-peeling algorithm is the most efficient among these methods. Numerical methods are applied, as a rule, to calculate $\kappa(z)$ from the desired spectral and dispersion responses of the grating. The reconstruction of the coupling coefficient of real gratings by these methods is hindered due to a complicated mathematical procedure, the ambiguity of

solutions obtained and the presence of noises in real spectra, which is especially inherent in gratings with high reflection coefficients.

To overcome these difficulties, several methods were proposed for complete or partial reconstruction of $\kappa(z)$ in real gratings by using additional principles for obtaining experimental data on their structure. Unfortunately, neither of these methods is universal (applicable for gratings of all types), which should be taken into account in the choice of the method for FBG diagnostics. The experimental methods proposed for FBG diagnostics are based on several main principles involving the detection of the following characteristics:

- (i) the intensity of radiation diffracted from a grating illuminated from the side;
- (ii) the variation in spectral characteristics caused by a local action on the grating;
- (iii) the intensity of incoherent Rayleigh scattering of radiation propagating in an optical fibre;
- (iv) the spectral and time response of gratings.

Diffraction methods for studying FBGs are described in Refs [16–18]. These methods use the fact that radiation incident of a grating through the side surface of an optical fibre undergoes diffraction from the grating. The intensity of diffracted radiation is uniquely related to the refractive-index modulation in the fibre core. Diffraction methods provide a high-precision measurement of the refractive-index modulation amplitude ($\Delta n_{\text{mod}} < 10^{-4}$) with a high spectral resolution ($\sim 10 \mu\text{m}$). By analysing additionally the interference of the zero and first diffraction orders, the authors of Ref. [18] obtained the spatial distribution of the period of a grating being tested. Because the diffraction method is comparatively simple and does not require sophisticated experimental equipment, it is often used to analyse the FBG structure. The main disadvantage of this method is strict requirements imposed on the purity of a fibre surface and mechanical stability of the elements of a measuring system, as well as the difficulty of obtaining the absolute value of $\Delta n_{\text{mod}}(z)$.

The heat scan and OSDR methods are based on the detection of a variation in the spectral response of a FBG subjected to a controllable local phase action on the grating structure. The heat scan method [19, 20] employs the local heating of a piece of a FBG, which results, due to a thermal expansion of the optical fibre and the thermo-optical effect, in the red shift of the local resonance wavelength. This method can be used for measuring either the local period of gratings with a variable period or the spatial distribution of the refractive-index modulation in gratings with a slowly varying period (within 0.1 %). However, although the heat scan method is quite simple, it has a poor spatial resolution ($\sim 0.5 \text{ mm}$) and a low accuracy of measurements. The OSDR method is also based on the induction of a local phase perturbation, but unlike the heat scan method, it uses a modulated local action, which qualitatively improves its characteristics.

The described methods allow the study of gratings with any (including high) reflection coefficient, whereas a common disadvantage of the methods described below is that the reflection coefficient of the FBG is bounded above for these methods. This is explained by the fact that, when the reflection coefficient is high, radiation at wavelengths near the resonance wavelength does not penetrate over the entire depth of the grating.

The methods for measuring the intensity of side Rayleigh scattering were used to find the distribution of the intensity of resonance radiation inside the grating [21]. When the spectrum of scattered radiation was additionally analysed, these methods were also used to determine the local period of the grating being tested [22]. The main drawbacks of these methods are their low sensitivity and a relatively low spatial resolution ($\sim 1 \text{ mm}$).

The detection of the spectral-time response of gratings is used in some methods, of which the most interesting ones employ a Michelson interferometer. In [23], a broadband radiation source was used for measurements, while in [24] a tunable laser was employed. In the first case, the dependence $\kappa(z)$ was obtained from a change in the optical length of the reference arm, while in the second case, this dependence was obtained by scanning the wavelength of testing radiation. These methods provide a high spectral resolution (0.1 nm and better) and a high sensitivity ($\Delta n_{\text{mod}} \sim 10^{-5}$). Their application is hindered in the case of gratings with sharp variations in the induced refractive index.

The authors of Ref. [25] proposed the frequency-temporal analysis of the pulsed response of a grating using the Wigner–Will distribution. However, this method allows the reconstruction of the grating period distribution only and requires the use of sophisticated equipment for the generation of stable pulses and reliable detection of the response.

3. Method of optical space-domain reflectometry

The OSDR method was first proposed in Ref. [26] for measuring the amplitude and phase of the coupling coefficient of a FBG. The method is based on the fact that a local phase perturbation at some point z_{meas} of the FBG causes a change in the grating spectrum, the value of this change being determined by the coefficient $\kappa(z_{\text{meas}})$. Therefore, the transmission coefficient T (or the reflection coefficient R) is a function of not only the wavelength but also of the induced phase Φ , as well as of the coordinate z_{meas} . A quantity being measured (the OSDR signal) is a variation in the transmission $T(\lambda, z, \Phi)$ [or reflection $R(\lambda, z, \Phi)$] at a fixed wavelength λ_{meas} , which is related to the local phase perturbation Φ by the expression

$$S(\lambda, z) = \frac{\partial T(\lambda, z, \Phi)}{\partial \Phi} \Phi = - \frac{\partial R(\lambda, z, \Phi)}{\partial \Phi} \Phi.$$

The spatial distribution of the OSDR signal is determined by scanning the phase perturbation along the grating being tested.

It was shown in Ref. [26] that the spatial derivative of the OSDR signal contains explicitly information on the amplitude and phase of the complex coupling coefficient of the grating:

$$\frac{\partial S(\lambda_{\text{meas}}, z)}{\partial z} = 2|r(\lambda_{\text{meas}})|\Phi|\kappa(z)|\cos[\phi_{\kappa}(z) + \phi_0(\lambda_{\text{meas}})], \quad (9)$$

where $r(\lambda_{\text{meas}})$ is the amplitude reflection coefficient of the grating at the measurement wavelength λ_{meas} ; $|r(\lambda)|^2 = R(\lambda)$; and $\phi_0(\lambda_{\text{meas}})$ is a constant depending mainly on the argument of the complex reflection coefficient $r(\lambda_{\text{meas}})$.

Expression (9) was obtained assuming that the reflection coefficient at the wavelength λ_{meas} is small (the contribution

from multiple reflections during the propagation of radiation in the grating is neglected) and the detuning of λ_{meas} from λ_0 is sufficiently large (i.e., the measurement is performed outside the main reflection peak [27]). Then, $2\pi L n_{\text{eff}} \Delta\lambda / \lambda_0^2 > [\pi^2 + (|\kappa|L)^2]^{1/2}$, where L is the grating length. From the practical point of view, these conditions mean that λ_{meas} should be chosen at one of the sidelobes in the grating spectrum. Note that the derivative of the OSDR signal is proportional namely to the amplitude reflection coefficient $r(\lambda_{\text{meas}})$, which can be for sidelobes several times greater than the reflection coefficient $R(\lambda_{\text{meas}})$ usually measured in experiments. One of the most important advantages of OSDR is the fact that the diagnostics of the grating is performed by measuring a change in reflection outside the resonance wavelength. This allows one to study gratings with high reflection coefficients, whereas other theoretical and experimental methods are restricted in this respect.

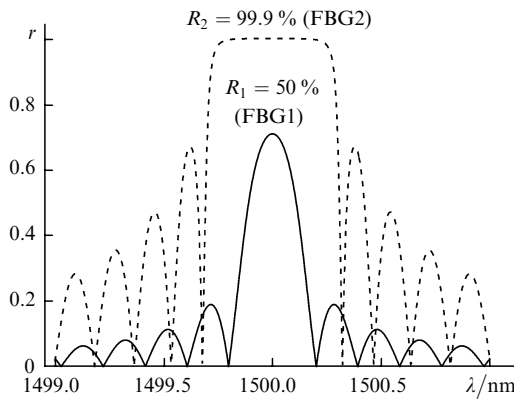


Figure 1. Amplitude reflection spectra of FBGs 1 and 2 with the reflection coefficients $R_1 = 50\%$ and $R_2 = 99.9\%$, respectively.

Consider the use of OSDR for the case of two homogeneous Bragg gratings 1 and 2 with substantially different reflection coefficients, whose dependences $r(\lambda)$ are presented in Fig. 1. The gratings have the parameters Δn_{mod} , Δn_{avr} and L , which are constant over the length $L = 4$ mm, and the resonance wavelength $\lambda_0 = 1500$ nm at which $\eta \approx 0.72$ for an optical fibre chosen for calculations. The modulation amplitude of the induced refractive index for gratings 1 and 2 is $\Delta n_{\text{mod}} = 3 \times 10^{-4}$ ($R = 50\%$) and 14×10^{-4} ($R = 99.9\%$), respectively.

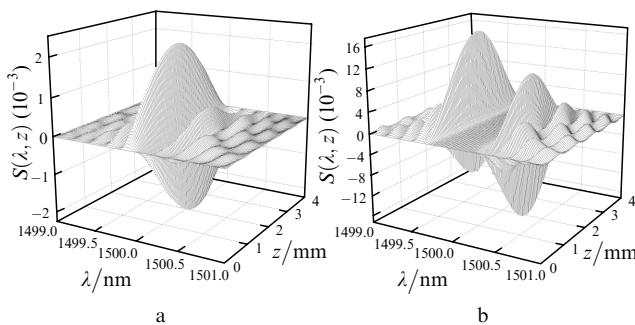


Figure 2. Dependences $S(\lambda, z)$ of the OSDR signal for FBG1 (a) and FBG2 (b).

Figs 2a, b show the calculated dependences of the spatial distribution of the OSDR signal on the wavelength for gratings 1 and 2, respectively, for the induced phase $\Phi = 10^{-2}$. The distribution of the OSDR signal is a periodic function of the coordinate z , the amplitude of spatial oscillations at a certain wavelength reproducing the dependence $r(\lambda)$ as a whole. In the case of a deep grating, the wavelength region with a high reflection coefficient is not manifested in the OSDR signal ($S \approx 0$, Fig. 2b) because the introduction of a relatively small phase perturbation Φ almost does not change reflection in this region. Note the important characteristic dependences of oscillations of the OSDR signal on the spectral detuning from λ_{Br} (Fig. 2). As the spectral detuning $|\Delta\lambda|$ is increased, the frequency of spatial oscillations increases, which improves the calculated accuracy of measurements and spatial resolution. However, the amplitude of oscillations decreases simultaneously, resulting in a decrease in the signal-to-noise ratio. Therefore, the optimal value of spectral detuning should be selected in each individual case using, for example, a tunable laser.

Note that the possibilities of OSDR are limited when special FBGs are used with a period strongly varying along the grating because in this case the intensity of the OSDR signal can be too small upon scanning of the parts of the grating having the resonance wavelength remote from λ_{meas} . In addition, problems can appear during diagnostics of gratings in which the intensity of sidelobes is considerably reduced by producing a special spatial distribution of the induced refractive index.

In Ref. [26], a local phase perturbation was induced in the fibre core using a helium-neon laser. Because of the weak absorption of this laser radiation by a silica glass, it was necessary to apply preliminary a special absorbing layer on a piece of the fibre with a grating being tested. In addition, the diffusion of heat along the fibre axis restricted the space-domain resolution of the method. In Ref. [28], we proposed to induce a local phase perturbation directly in the fibre core by IR radiation from a CO laser or UV radiation of the second harmonic from an argon laser. This made it possible to avoid the deposition of an additional absorbing coating on the fibre, to improve the spatial resolution (~ 100 μm)

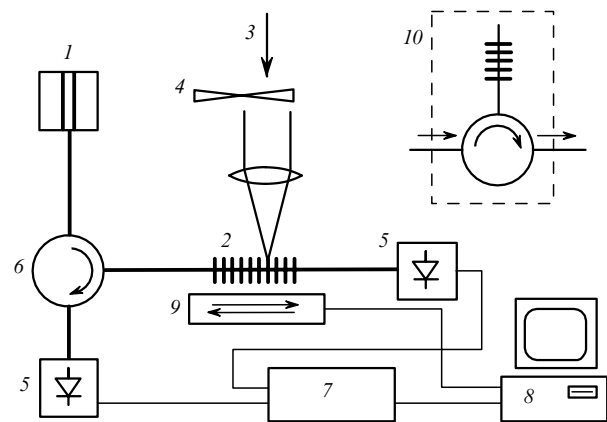


Figure 3. Scheme of the OSDR setup: (1) semiconductor laser; (2) FBG being tested; (3) phase-inducing laser radiation; (4) modulator of phase-inducing radiation; (5) photodetector; (6) fibre circulator; (7) lock-in amplifier; (8) computer; (9) mechanical translator; (10) unit for spectral filtration of a signal.

and the homogeneity of perturbation over the core radius, as well as to enhance the sensitivity of the method due to a large amplitude Φ of the phase perturbation.

The scheme of the OSDR setup used in our experiments is shown in Fig. 3. Radiation from a semiconductor laser (1) at the wavelength λ_{meas} , which was chosen based on the principles discussed above, entered into an optical fibre with grating (2) being tested. Laser radiation (3) modulated at the frequency f induced a local phase perturbation in the grating. Variations in the transmission or reflection spectra of the grating were detected with photodetector (5). In reflection measurements, which are preferable because they allow one to exclude the intense constant component, a fibreoptic circulator (6) was used. The OSDR signal was measured at the modulation frequency f using a lock-in amplifier (7), the fibre with the grating being moved at a constant speed ($\sim 1 \text{ mm min}^{-1}$) using mechanical translator (9) controlled with computer (8).

Synchronous detection of a signal enhances the sensitivity of measurements, which allows the use of relatively low-power UV and IR radiation, which does not cause any significant irreversible variations in the grating structure.

Phase perturbations were induced by the $\sim 5\text{-}\mu\text{m}$ radiation from a CO laser and the 244-nm radiation of the second harmonic from an argon laser [(3) in Fig. 3]. Both these radiations are capable of inducing a sufficiently large phase perturbation, which, as follows from (9), enhances the sensitivity of the method.

IR radiation from the CO laser penetrates into a silica glass by 100–200 μm , which is comparable with the diameter of the fibre cladding (125 μm). This provides a sufficiently uniform heating of the fibre over its cross section, thereby inducing, due to the thermo-optical effect, an additional refractive index. Radiation from a CO laser was focused on the fibre with a fluorite lens into a spot of diameter $\sim 150 \mu\text{m}$. The characteristic time of the fibre cooling was $\sim 0.1 \text{ s}$, which restricted the possibility of increasing the modulation frequency f . For this reason, this frequency was chosen to provide the maximum signal-to-noise ratio for the OSDR signal and was 230 Hz. In this case, the constant component of the induced phase perturbation was $\sim 0.14 \text{ rad}$, while the modulation component was an order of magnitude lower. The phase shift in the grating, taking into account the length of the irradiated part of the fibre, allows one to estimate the heating of the fibre in the region of its irradiation. In our case, the temperature increase was $\sim 30 \text{ K}$, which is much lower than the degradation temperature of the photoinduced refractive index.

The UV radiation can induce both irreversible and reversible variations in the refractive index in the core of a germanium-doped optical fibre [29]. The main mechanisms of reversible variations are excitation of germanium oxygen-deficient centres, which are accompanied by a change in the glass polarisability, and the heating of the core glass due to the nonradiative relaxation of excited centres. The constant component of the local phase perturbation during the testing of gratings, as in the case of the CO laser, was $\sim 0.1 \text{ rad}$. The UV radiation was focused into a spot of diameter $\sim 50 \mu\text{m}$ providing a power density of $\sim 30 \text{ W cm}^{-2}$, which, taking the movement velocity into account, corresponded to the total irradiation fluence $\sim 500 \text{ J cm}^{-2}$ per transit. This fluence corresponds to the induced irreversible variation in the refractive index $\Delta n \sim 10^{-5}$ in an SMF-28

fibre, which is much lower than the average refractive index $\Delta n \sim 10^{-3}$ induced during the manufacturing of tested FBGs. Nevertheless, this irreversible variation in the refractive index in the fibre induced by UV light makes IR radiation from a CO laser preferable.

Note also that, when a fibre is exposed to UV light, the measurements are hindered due to excitation of photoluminescence with a maximum at $\sim 400 \text{ nm}$, which has the same modulation frequency and can be detected by a broadband photodetector. We solved this problem by placing directly in front of photodetector (5) an additional FBG (in measurements both in transmission and reflection) (Fig. 3), which reflected light at the wavelength λ_{meas} , together with fibreoptic circulator (10).

We tested FBGs with high reflection coefficients, which were written in a standard single-mode SMF-28 optical fibre loaded with molecular hydrogen. The gratings were written by the 244-nm second harmonic of an argon laser in a Lloyd interferometer (see section 3.1.6 in Ref. [1]) and had a length of $\sim 5 \text{ mm}$.

4. Results and discussion

Fig. 4 shows the spatial distributions of the OSDR signal for one of the tested FBGs, which were measured for two detunings of λ_{meas} from λ_{Br} . One can see that the grating is located on a piece of length $\sim 5 \text{ mm}$, where the oscillations of the OSDR signal are observed ($1 \text{ mm} < z < 6 \text{ mm}$). The amplitude of the oscillations decreases with increasing detuning and their number increases, corresponding to the regularity noted above (see Fig. 2).

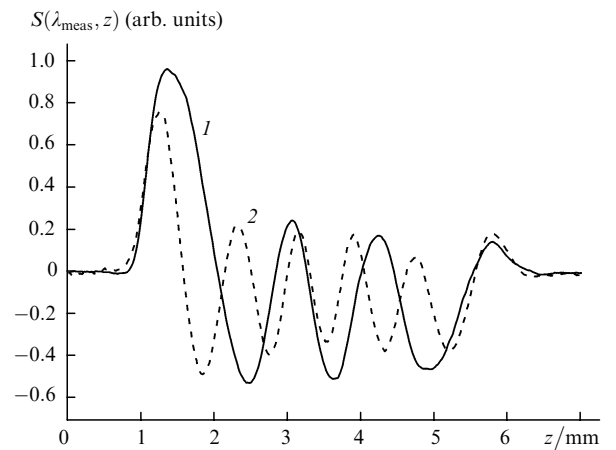


Figure 4. Spatial distributions of the OSDR signal measured at spectral detunings 0.9 (1) and 1.5 nm (2).

The distribution of the coupling coefficient $\kappa(z)$ of the grating was found from Eq. (9) after the differentiation of $S(\lambda_{\text{meas}}, z)$ with respect to z . We used in calculations the fact that the complex representation of the function can be reconstructed based on the distribution of its real part [the right part in (9)] assuming that the amplitude and frequency slowly vary during the oscillation period. For this purpose, it is sufficient to set equal to zero the values in the region of negative frequencies in the spectrum of the function obtained by the direct Fourier transform and then to perform the inverse Fourier transform.

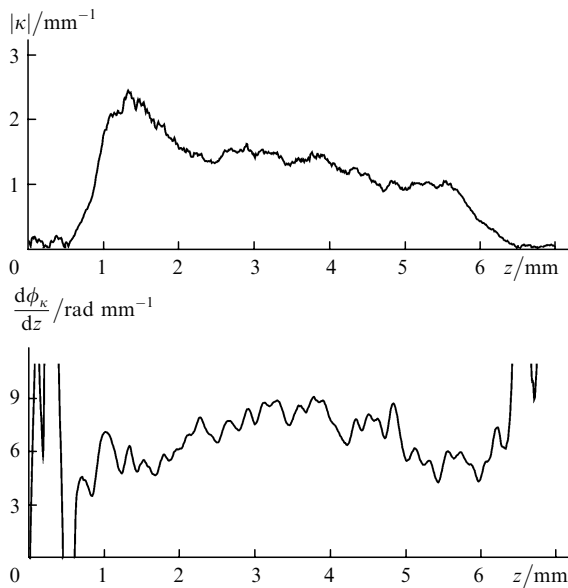


Figure 5. Amplitude and derivative of the phase of the complex coupling coefficient of a grating.

As a result of this procedure applied to the function $\partial S(\lambda_{\text{meas}}, z)/\partial z$, the spatial distributions $|\kappa(z)|$ and $\phi_{\kappa}(z)$ were obtained explicitly. Fig. 5 shows the functions $|\kappa(z)|$ and $d\phi_{\kappa}(z)/dz$ obtained after the processing of experimental data presented in Fig. 4 [curve (2)]. The absolute values of the modulus of the coupling coefficient were calculated by comparing the experimental transmission spectrum of the grating with the spectrum calculated taking into account the obtained values of $\kappa(z)$.

Fig. 6 shows the distribution $\Delta n_{\text{mod}}(z)$ for one of the tested FBGs, which was measured by the OSDR method using IR [curve (1)] and UV [curve (2)] radiation sources. Also, the distribution measured by the method of side diffraction [16] is presented [curve (3)]. The coincidence (with an accuracy of 10%–15%) between these curves demonstrates the reliability of the results and gives the estimate of the accuracy of measurement of $\Delta n_{\text{mod}}(z) \sim 10^{-4}$. An asymmetric shape of this distribution,

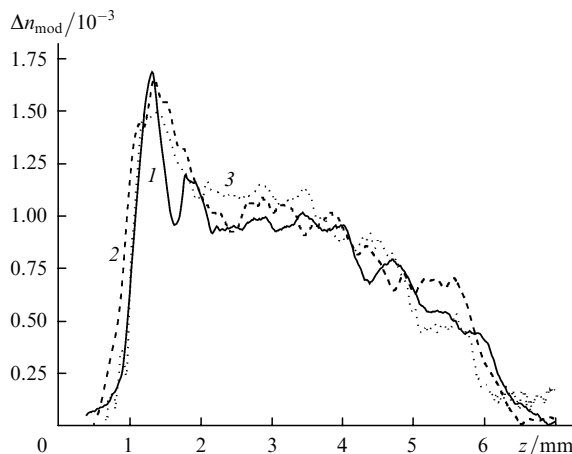


Figure 6. Distributions of the modulation amplitude of the refractive index calculated from the data measured by the UV OSDR (1), IR OSDR (2) and side diffraction (3) methods.

which rather sharply increases in the region $z = 1$ mm and smoothly decreases from the other side of the grating, is explained by the distribution of the intensity of UV radiation used for FBG writing.

Consider phase information contained in the coupling coefficient in accordance with Eqn (8). The first term in the right-hand part of (8) is determined by the detuning of the measurement wavelength from the resonance wavelength of the grating. It is independent of the coordinate z and is an average value of the phase derivative. The value of this term for the data presented in Fig. 5 is ~ 6 rad mm^{-1} , in good agreement with one oscillation period (2π) of the OSDR signal over the length 1 mm [Fig. 4, curve (2)]. Spatial variations of the phase derivative are determined by two other terms in Eqn (8), namely, by variations $\delta n_{\text{ind}}(z)$ in the induced refractive index and the grating period $\delta A(z)$. To separate the contributions from these parameters, it is necessary to introduce additional assumptions, for example, about the contrast of the pitches of the grating under study (the ratio $\Delta n_{\text{mod}}/\Delta n_{\text{avr}}$) or perform measurements for several gratings written by using different UV exposure doses. In the latter case, we should use the fact that, unlike $\delta n_{\text{ind}}(z)$, the period of the grating is independent of the exposure dose.

Using the measured values of $\kappa(z)$, we calculated the transmission spectra of the grating and compared them with the spectrum measured using an HP-70950B spectrum analyser (Fig. 7). The comparison was performed within the dynamic range of measurements taking into account the spectral width of the instrumental function of the spectrum analyser ($\Delta\lambda \sim 0.08$ nm). One can see that the transmission spectrum calculated using the measured distribution of the modulation amplitude $\Delta n_{\text{mod}}(z)$ of the refractive index neglecting the phase of the coupling coefficient $\phi_{\kappa}(z)$ [curve (3)] does not agree well enough with the experimental spectrum [curve (1)], whereas the spectrum calculated taking into account the phase [curve (2)] is in much better agreement with the experiment.

Along with the transmission and reflection spectra, the data on the amplitude and phase of the coupling coefficient of the FBG allow one to calculate the group delay and dispersion of gratings [10]. Fig. 8 presents these characteristics for the grating whose coupling coefficient is presented

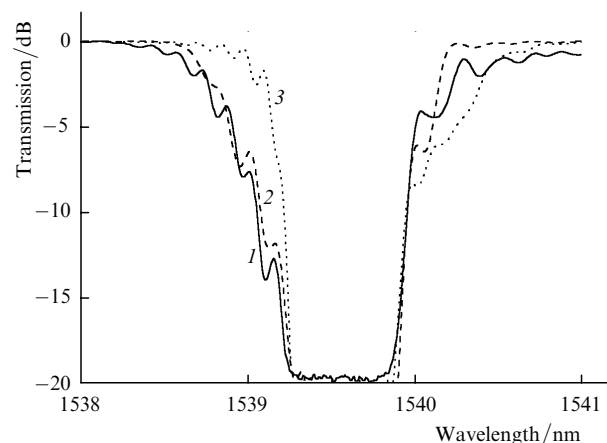


Figure 7. Transmission spectrum of the tested FBG (1) and transmission spectra calculated taking into account the amplitude and phase of the coupling coefficient (2) and only the amplitude (3).

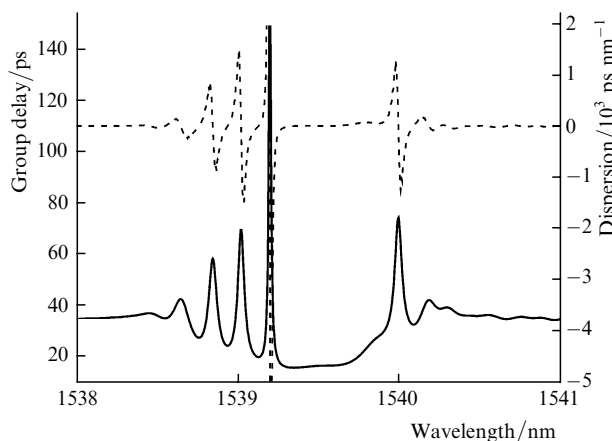


Figure 8. Group delay (solid curve) and dispersion (dashed curve) of the tested FBG.

in Fig. 5. Such a possibility of estimating dispersion characteristics of gratings is quite useful because their measurement is a separate and rather complicated technical problem.

Note that the calculation of spectral and dispersion characteristics of gratings from the data obtained by the OSDR method allows one to refine sometimes these characteristics when they cannot be accurately measured because of experimental limitations such as an inadequate spectral resolution or an inadequate dynamic range of measurements.

5. Conclusions

We have performed a comparative analysis of the main methods for measuring spatial characteristics of FBGs and described in detail the OSDR method used to measure the spatial distribution of the complex coupling coefficient. The experiments performed with IR (CO laser) and UV (second harmonic of an argon laser) radiation sources have shown that the method provides good sensitivity of measurements of the induced refractive index in the core of an optical fibre ($\sim 10^{-4}$) and a high spatial resolution ($\sim 100 \mu\text{m}$ and better). We have shown that this method allows one to avoid in some cases the restrictions imposed on the resolution and dynamic range by spectral instruments used in measurements and to calculate the dispersion characteristics of gratings.

Acknowledgements. The authors thank E. Brinkmeyer, F. Knappe, and H. Renner of the Technical University of Hamburg for useful discussions of the results and M.V. Grekov (FORC, GPI, RAS) for his help in the experimental study. This work was partially supported by the Russian Foundation for Basic Research (Grant No. 00-15-96650).

References

1. Kashyap R. *Fiber Bragg Gratings* (San Diego, Cal.: Academic, 1999).
2. Othonos A., Kalli K. *Fiber Bragg Gratings: Fundamentals and Applications in Telecommunications and Sensing* (Norwood, Mass.: Artech House, 1999).
3. Neustruev V.B. *J. Phys. Condens. Matter*, **6**, 6901 (1994).
4. Vasiliev S.A. *Proc. SPIE Int. Soc. Opt. Eng.*, **4357**, 1 (2001).
5. Lemaire P., Atkins R.M., Mizrahi V., Reed W.A. *Electron. Lett.*, **29**, 1191 (1993).
6. Dianov E.M., Prokhorov A.M. *IEEE J. Sel. Top. Quantum Electron.*, **6**, 1022 (2000).
7. Archambault J.-L., Grubb S.G. *J. Lightwave Technol.*, **15**, 1378 (1997).
8. Litchinitser N.M., Patterson D.B. *J. Lightwave Technol.*, **15**, 1323 (1997).
9. Canning J., Sceats M.G. *Electron. Lett.*, **30**, 1244 (1994).
10. Erdogan T. *J. Lightwave Technol.*, **15**, 1277 (1997).
11. Roman J.E., Winick K.A. *IEEE J. Quantum Electron.*, **29**, 975 (1993).
12. Brinkmeyer E. *Opt. Lett.*, **20**, 810 (1995).
13. Fedec R., Zervas M.N., Muriel M.A. *IEEE J. Quantum Electron.*, **35**, 1105 (1999).
14. Froggatt M. *Appl. Opt.*, **35**, 5162 (1996).
15. Song G.H., Shin S.Y. *J. Opt. Soc. Am. A*, **2**, 1905 (1985).
16. Krug P.A., Stolte R., Ulrich R. *Opt. Lett.*, **20**, 1767 (1995).
17. Ramecourt D., Bernage P., Niay P., Douay M., Riant I. *Bragg Gratings, Photosensitivity, and Poling in Glass Waveguides. OSA Tech. Dig.* (Washington, DC: OSA, 2001) Paper BThC8.
18. El-Diasty F., Heaney A., Erdogan T. *Appl. Opt.*, **40**, 890 (2001).
19. Sandgren S., Sahlgren B., Asseh A., Margulis W., Laurell F., Stubbe R., Lidgard A. *Electron. Lett.*, **31**, 665 (1995).
20. Roussel N., Magne S., Martinez C., Ferdinand P. *Opt. Fiber Technol.*, **5**, 119 (1999).
21. Canning J., Psaila D.C., Brodzeli Z., Higley A., Janos M. *Appl. Opt.*, **36**, 9378 (1997).
22. Canning J., Janos M., Stepanov D.Yu., Sceats M.G. *Electron. Lett.*, **32**, 1608 (1996).
23. Lambelet P., Fonjallaz P.Y., Limberger H.G., Salathe R.P., Zimmer C., Gilgen H.H. *IEEE Photon. Tech. Lett.*, **5**, 565 (1993).
24. Huang D., Yang C. *Appl. Opt.*, **38**, 4494 (1999).
25. Azana J., Muriel M.A. *J. Opt. Soc. Am. A*, **17**, 2496 (2000).
26. Brinkmeyer E., Stolze G., Johlen D. *Bragg Gratings, Photosensitivity, and Poling in Glass Fibers and Waveguides: Applications and Fundamentals. OSA Tech. Dig.* (Washington, DC: OSA, 1997) Vol.17, pp 33–35.
27. Kashyap R. *Opt. Fib. Technol.*, **1**, 17 (1994).
28. Korolev I.G., Vasiliev S.A., Medvedkov O.I., Dianov E.M., Knappe F., Knothe Ch., Renner H., Brinkmeyer E. *Bragg Gratings, Photosensitivity, and Poling in Glass Waveguides. OSA Tech. Dig.* (Washington, DC: OSA, 2001) Paper BWA2.
29. Danailov M.B., Gasmi T., Apai P. *Electron. Lett.*, **32**, 482 (1996).